

## Force Barriers for Membrane Tube Formation

Gerbrand Koster,<sup>1</sup> Angelo Cacciuto,<sup>1</sup> Imre Derényi,<sup>2</sup> Daan Frenkel,<sup>1</sup> and Marileen Dogterom<sup>1</sup>

<sup>1</sup>*FOM Institute for Atomic and Molecular Physics (AMOLF), Kruislaan 407, 1098 SJ Amsterdam, The Netherlands*

<sup>2</sup>*Department of Biological Physics, Eötvös University, Pázmány P. stny. 1A, H-1117 Budapest, Hungary*

(Received 15 July 2004; published 16 February 2005)

We used optical tweezers to measure the force-extension curve for the formation of tubes from giant vesicles. We show that a significant force barrier exists for the formation of tubes, which increases linearly with the radius of the area on which the pulling force is exerted. The tubes form through a first-order transition with accompanying hysteresis. We confirm these results with Monte Carlo simulations and theoretical calculations. Whether membrane tubes can be formed in, for example, biological cells, thus depends on the details of how forces are applied.

DOI: 10.1103/PhysRevLett.94.068101

PACS numbers: 87.16.Dg, 87.68.+z

Lipid bilayer membranes are essential for the compartmentalization of cells. A ubiquitously present shape is the membrane tube. New membrane tubes are formed from the Golgi apparatus as precursors for transport intermediates [1] and the characteristic morphology of the endoplasmic reticulum is dynamically maintained by the constant formation and retraction of membrane tubes [2]. In addition, membrane tubes have been shown to interconnect separate cells [3]. Different force generating processes like the movement of motor proteins and the polymerization of cytoskeletal filaments have been suggested to be responsible for tube formation in cells [4]. For a better understanding of the relevant physics involved in tube formation, several experimental techniques have been used to pull tubes from cell membranes and synthetic vesicles. These techniques include hydrodynamic flow [5], micropipettes [6], optical and magnetic tweezers [7–11], and also motor proteins and polymerizing microtubules [10–12]. Most studies have either focused on the static force of extended tubes, or have examined dynamic effects that occur when elongating tubes at high speeds [13].

The force that determines in practice, however, whether a tube can be formed, is the force barrier connected with the initial deformation of the membrane. Recent theoretical studies have focused on the different shapes a membrane assumes when a force is applied to a single point [14–16] (see also [17]). They show that the force required for moving the point away increases while the membrane is being deformed. At a certain extension a transition to a configuration with a less deformed membrane and a tubular protrusion occurs. This conformation requires a lower plateau force,  $F_0$ , to be maintained. The value of the overshoot force (the force barrier for tube formation),  $F_{\text{over}}$ , was predicted to be  $\sim 13\%$  higher than  $F_0$  [14,16]. Under certain conditions, the shape transition was furthermore predicted to be discontinuous (first order) [15,16,18]. In reality, a force is, however, never applied to a single point as was assumed in these theoretical studies. When using beads to pull tubes, a certain number of molecular links will be formed between the membrane and the bead, cor-

responding to a finite attachment area. The same is true in living cells, where (clusters of) molecular motors are expected to occupy an area that may be of significant size.

In this Letter, we present data on the force-extension curve for membrane tube formation. Our experiments with optical tweezers demonstrate the existence of a force barrier and show that a finite attachment area (patch size) significantly increases the value of the force overshoot. The data show a linear increase of the force overshoot with the patch radius,  $R_p$ . We confirm our results with simulations and theoretical calculations.

To measure the force-extension curve of a membrane tube we first immobilized a biotinylated giant vesicle [19] on a cover slip with a streptavidin coated polystyrene bead [20]. Subsequently, another bead was taken and the stiffness of the tweezers was determined from a power spectrum [21]. This bead was brought into contact with the vesicle for a short time with the tweezers. Next the vesicle was moved away with a piezoelectric stage for 10–15  $\mu\text{m}$  at a constant velocity (0.5  $\mu\text{m/s}$ ) and a tube was formed (see Fig. 1). Pulling faster resulted in a significant dynamic component in the force (data not shown). The force on the bead was determined by “template tracking” of the differential interference contrast (DIC) microscopy images to measure the deviation of the bead position from the trap center [22]. During initial bead-vesicle separation the force on the bead increased [Fig. 2(b)], until at a certain (patch-size-dependent) displacement and force, a transition occurred from a vesicle in a deformed state to a more spherical vesicle with a tube. At this geometrical phase transition the force dropped to a lower plateau value. Overshoot forces that are much larger (up to 40 pN) than the plateau value ( $\sim 4$  pN for this vesicle) were observed [Fig. 2(b)]. Next, the vesicle and bead were moved toward each other again. During this retraction we observed a much smaller “retraction overshoot”, due to the hysteresis effect for a first-order transition that was predicted [15,16]. After each retraction, the bead was pushed against the vesicle again for several seconds, so that more biotin-streptavidin bonds could be created between the vesicle and the bead. This

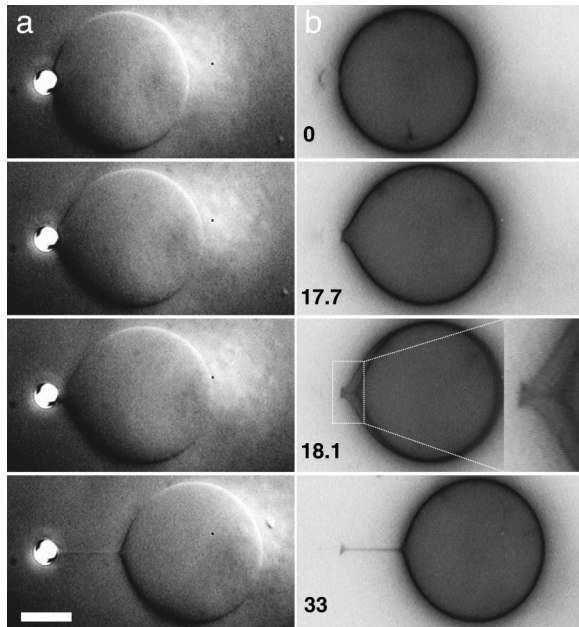


FIG. 1. Tube formation from a vesicle. (a) Snapshots from DIC microscopy. From top to bottom: a vesicle in a spherical state when no force is exerted on it, the vesicle deformed with the tweezers, the transition point, and a vesicle with a tube. (b) Inverted contrast fluorescence images of the same vesicle. By integrating the signal (160 ms), we can observe the overlapping image of the vesicle just before and just after tube formation in the third picture from the top. The zoom in this picture shows that the attachment area does not change during tube formation. Time is in seconds. Scale bar:  $10 \mu\text{m}$ .

frequently resulted in an increase in patch size [Fig. 2(a)], and a corresponding increase of the overshoot force for following tube formations [Fig. 2(b)]. Since the patch itself was not visible with DIC microscopy, we used fluorescence microscopy to evaluate the patch size each time after a tube had formed. Figure 2(a) shows inverted contrast fluorescence images of tubes with different patch sizes formed from the same vesicle. We determined the patch radius by drawing a straight vertical line along the patch and counting the pixels. Depending on the quality of the image, we estimate that this results in 2–4 pixels ( $\sim 150\text{--}300 \text{ nm}$ ) uncertainty on the patch radius. To study the relationship between the patch size and the value of the force overshoot, we plot the overshoot values versus the patch radius,  $R_p$ , for different vesicles in Fig. 2(c). At  $R_p = 0$  the value of the plateau force is plotted, which is close to the force overshoot expected for a point force. The data suggest a linear dependence of the force overshoot on the patch radius, with a slope that is higher for larger plateau forces. Higher plateau forces correspond to higher tensions (see below), which are slightly different between different vesicles [10]. The relative errors on the overshoot forces (not shown) are small (from  $\sim 2\%$  for large forces to  $\sim 10\%$  for smaller forces) because the displacements corresponding to these forces are high compared to the noise in the bead position.

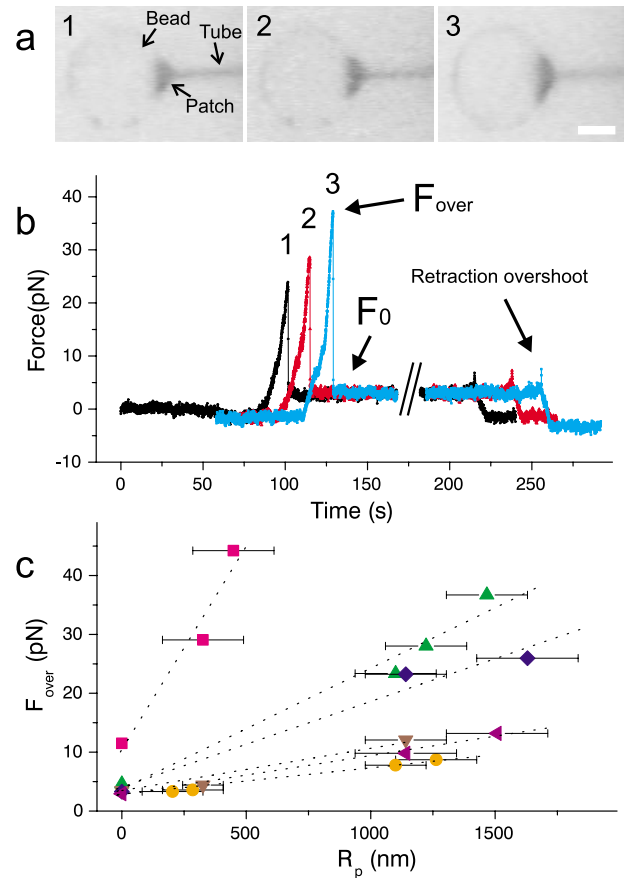


FIG. 2 (color online). Subsequent tube pulls from the same vesicle. (a) Inverted contrast fluorescence images of an increasing attachment area after subsequent tube pulls. Scale bar:  $2 \mu\text{m}$ . (b) The force on the bead during tube formation for the different pulls. The three curves correspond to the three patches in (a). In each pull the stage is moved for 20 s ( $10 \mu\text{m}$ ) during which the force grows until at  $F_{\text{over}}$  a tube is formed and the force drops to  $F_0$ . After the stage movement has stopped, the patch size is evaluated in fluorescence (at the break), and subsequently the stage is moved back  $10 \mu\text{m}$  while the tube retracts. (c) The overshoot force as a function of the radius of the patch ( $R_p$ ) for six different vesicles. The larger slopes correspond to vesicles with higher plateau forces (which are plotted at  $R_p = 0$ ). The dotted lines are linear fits to the data.

To check our experimental results, we performed Monte Carlo simulations of tube formation (Fig. 3), using a simple model for a fluid membrane [23]. The model consists of  $N$  hard spheres, of diameter  $a$ , connected by flexible links to form a triangulated network [24] whose connectivity is dynamically rearranged to simulate the fluidity of the membrane [23]. The simulations also show that the overshoot force increases with patch size [Fig. 3(b)]. By analyzing the force needed to form a tube as a function of the radius of the patch we again find a linear behavior (for patches larger than the tube diameter), where the slope increases with membrane tension [Fig. 3(c)].

Before the tube formation transition, the shape of the membrane is best described by a catenoid [14,16,18] super-

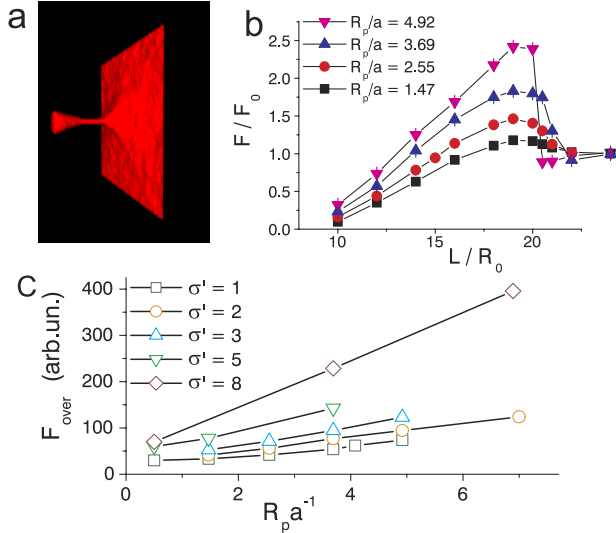


FIG. 3 (color online). Overshoot forces from the Monte Carlo simulations. (a) Graphical representation of a tube pulled in a simulation. (b) Force-extension curves for different patch sizes. The extension,  $L$ , is normalized to the tube radius ( $R_0$ ). (c) The overshoot force as a function of the patch radius for membranes with several relative surface tensions ( $\sigma'$ ).

imposed on the sphere of the vesicle. In our experiments the end ring of this catenoid can be identified as the rim of the patch, and it can support forces up to about  $2\pi R_p \sigma = 0.5F_0 R_p/R_0$ . When the pulling force exceeds this value, the membrane collapses onto a tube of radius  $R_0$ . Thus, the ratio between the radii of the patch and the tube is expected to determine the overshoot force relative to the plateau force. To be able to correctly impose the zero contact angle boundary condition at the rim of the patch, we have also solved the shape equations numerically [16], which predicts the more accurate  $F_{\text{over}}/F_0 = 1 + 0.5R_p/R_0$  asymptotic dependence in the large  $R_p$  limit. When properly normalized, our simulation results in fact confirm this prediction (Fig. 4).

To establish whether our experimentally measured overshoot forces are also consistent with this prediction, we normalized the patch size with respect to the radius of the tube and the overshoot force with respect to the plateau force (Fig. 4). The radius of the tube is below the resolution of the microscope, but it can be derived from the plateau force. The plateau force and the radius of the tube are both determined by the membrane tension,  $\sigma$ , and the bending rigidity,  $\kappa$ , of the membrane  $F_0 = 2\pi\sqrt{2\sigma\kappa}$  and  $R_0 = \sqrt{\kappa/2\sigma}$ , [13,16]. Taken together these yield  $R_0 = 2\pi\kappa/F_0$ . Since the bending rigidity for the vesicles used in our experiments has not been measured, we took the bending rigidity of 85 pN nm for pure 1,2-di-oleoyl-sn-glycero-3-phosphocholine (DOPC) vesicles [25]. Because of the limited force the tweezers can exert, we use vesicles with a relatively low plateau force ( $\sim 5$  pN). This allows us to measure the high force barriers of tubes with patches of resolvable size. The total error on the ratio between  $R_p$  and

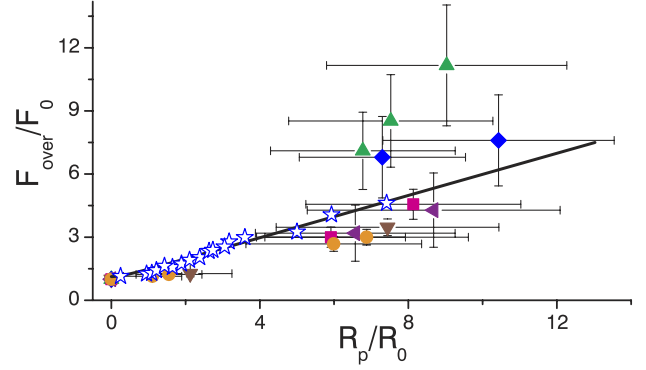


FIG. 4 (color online). The relative overshoot versus the patch radius normalized with the radius of the tube. The experimental data are consistent with the results from the Monte Carlo simulations (blue open stars) and the theoretical calculations (black line).

$R_0$  (see Fig. 4) is relatively large. This is due to a combination of measurement errors on the patch size and the low plateau force ( $\sim 20\%$ ), and a systematic uncertainty in the bending rigidity. Despite this, the experimental data are, without any fitting parameters, consistent with the theoretical prediction and the results from the simulations.

It has to be noted that in the simulations and in the theoretical calculations the surface tension is kept constant, whereas in our experiments we do not control the tension. It is expected that the tension increases with area extension as thermal fluctuations are smoothed out [26]. This increase in tension should be present when the membrane is deformed before tube formation, but also when a short membrane tube is elongated. We estimate that a comparable increase in area (0.5%) is expected for the formation of a  $\sim 10$   $\mu\text{m}$  tube of a radius of 100 nm as for the formation of the catenoid that is present before tube formation (for a patch size of  $\sim 1$   $\mu\text{m}$ ). This should in principle increase the tension by about a factor of 10 [26] and the plateau force by about  $\sqrt{10}$ . However, in most experiments we do not observe a significant increase in the plateau force when elongating a tube, suggesting that a “reservoir” of membrane area must be present, which effectively keeps the surface tension constant. This reservoir may consist of smaller membrane inclusions [27] that can get incorporated in the vesicle membrane when the tension grows, or may be due to the partial detachment of the membrane from the cover slip surface [17]. In some experiments the catenoidal shape that is formed before tube formation may require an area that the reservoir is not able to supply, in which case the tension will increase. This may explain why we find higher than theoretically expected overshoot forces for one of the vesicles (Fig. 4). Another reason for the deviation of individual data could be an initial tension imbalance between the two leaflets of the bilayer. This would create a nonlocal elasticity and affect the value of  $F_0$ , leading to an under- or overestimation of  $F_{\text{over}}/F_0$ . However, as the vesicles have a quasi-

spherical shape initially, this contribution is expected to be small.

In conclusion, we have shown that the force barrier for the formation of a membrane tube grows linearly with the size of the area the force is exerted on. These results should be taken into account in studies where the tube formation force is used to characterize mechanical properties of (cell) membranes [8,9]. For example, in Li *et al.* tubes that were formed from different sides of a cell resulted in different overshoot forces [9]. It was concluded that this was due to differences in the cytoskeletal cortex, whereas differences in patch size due to the affinity for the probing bead could have also affected this result.

The dependence on the patch size for the formation of tubes may be relevant for controlled intracellular membrane tube formation. In cells, lipid subdomains of a (few) hundred nm size [28] as well as clusters of proteins [29] are found on the membrane. When a tube must be formed by exerting a force on one of these “patches” [30], the force required for the initial step in the formation of the tube may be too high for the force generator (e.g., kinesin, polymerizing cytoskeletal elements) to overcome. The acquisition of proteins or lipids that can help the initial curvature [29,31] may be required to lower the overshoot force. Once a tube is formed the force is lower and regular force generators could take over.

We thank M. van Duijn, J. Kerssemakers, P. Bassereau, R. Merkel, P. Nassoy, and E. Evans for helpful comments, and M. Bonn for a critical reading of the manuscript. This work is part of the research program of the “Stichting voor Fundamenteel Onderzoek der Materie (FOM)”, which is financially supported by the “Nederlandse organisatie voor Wetenschappelijke Onderzoek (NWO)” I.D. acknowledges support from the Hungarian Science Foundation (Grant No. OTKA F043756) and a Marie Curie European Reintegration Grant (No. 505969).

- 
- [1] N. Sciaky *et al.*, J. Cell Biol. **139**, 1137 (1997); E. V. Polishchuk, A. Di Pentima, A. Luini, and R. S. Polishchuk, Mol. Biol. Cell **14**, 4470 (2003).
- [2] C. Lee and L. B. Chen, Cell **54**, 37 (1988).
- [3] A. Rustom *et al.*, Science **303**, 1007 (2004).
- [4] R. D. Vale and H. Hotani, J. Cell Biol. **107**, 2233 (1988); C. M. Waterman-Storer and E. D. Salmon, Curr. Biol. **8**, 798 (1998).
- [5] R. E. Waugh, Biophys. J. **38**, 29 (1982).
- [6] E. Evans *et al.*, Science **273**, 933 (1996).
- [7] V. Heinrich and R. E. Waugh, Ann. Biomed. Eng. **24**, 595 (1996).
- [8] D. Raucher and M. P. Sheetz, Biophys. J. **77**, 1992 (1999); T. Roopa and G. V. Shivashankar, Appl. Phys. Lett. **82**, 1631 (2003); H. Hotani *et al.*, BioSystems **71**, 93 (2003); A. Upadhyaya and M. P. Sheetz, Biophys. J. **86**, 2923 (2004).
- [9] Z. Li *et al.*, Biophys. J. **82**, 1386 (2002).
- [10] G. Koster, M. VanDuijn, B. Hofst, and M. Dogterom, Proc. Natl. Acad. Sci. U.S.A. **100**, 15 583 (2003).
- [11] D. K. Fygenson, J. F. Marko, and A. Libchaber, Phys. Rev. Lett. **79**, 4497 (1997).
- [12] A. Roux *et al.*, Proc. Natl. Acad. Sci. U.S.A. **99**, 5394 (2002).
- [13] E. Evans and A. Yeung, Chem. Phys. Lipids **73**, 39 (1994).
- [14] T. R. Powers, G. Huber, and R. E. Goldstein, Phys. Rev. E **65**, 041901 (2002).
- [15] V. Heinrich, B. Bozic, S. Svetina, and B. Zeks, Biophys. J. **76**, 2056 (1999).
- [16] I. Derenyi, F. Julicher, and J. Prost, Phys. Rev. Lett. **88**, 238101 (2002).
- [17] A. S. Smith, E. Sackmann, and U. Seifert, Phys. Rev. Lett. **92**, 208101 (2004).
- [18] V. A. Frolov *et al.*, Proc. Natl. Acad. Sci. U.S.A. **100**, 8698 (2003).
- [19] The vesicles were made by the electroformation method [10]. They consisted of 96.7 mol% DOPC (1,2-di-oleoyl-sn-glycero-3-phosphocholine), 3.1 mol% 1,2-di-oleoyl-sn-glycero-3-phosphoethanolamine-N-(Cap Biotinyl), and 0.2 mol% (fluorescent) rhodamine labeled DOPE [1,2-di-oleoyl-sn-glycero-3-phosphoethanolamine-N-(Cap Biotinyl)] (Avanti Polar Lipids).
- [20] In an isoosmotic buffer of 112 mM Glucose, 40 mM Pipes, 4 mM MgCl<sub>2</sub>, 1 mM EGTA, 4 mM DTT, 0.2 mg/ml catalase and 0.4 mg/ml glucose oxidase, a bead (SVP-40-5, Spherotech, Libertyville, IL) was held against the vesicle and a strong (big patch) connection was made. This bead was nonspecifically attached to a coverslip, which was coated with 2.5 mg/ml  $\alpha$ -casein to prevent the vesicles from exploding on the glass surface.
- [21] K. Visscher, S. P. Gross, and S. M. Block, IEEE J. Sel. Top. Quantum Electron. **2**, 1066 (1996).
- [22] C. Faivre-Moskalenko and M. Dogterom, Proc. Natl. Acad. Sci. U.S.A. **99**, 16 788 (2002).
- [23] J.-S. Ho and A. Baumgärtner, Europhys. Lett. **12**, 295 (1990); A. Baumgärtner and J.-S. Ho, Phys. Rev. A **41**, 5747 (1990).
- [24] Y. Kantor, M. Kardar, and D. R. Nelson, Phys. Rev. Lett. **57**, 791 (1986).
- [25] W. Rawicz *et al.*, Biophys. J. **79**, 328 (2000).
- [26] E. Evans and W. Rawicz, Phys. Rev. Lett. **64**, 2094 (1990).
- [27] W. Helfrich, in *Structure and Dynamics of Membranes*, edited by R. Lipowsky and E. Sackmann (Elsevier Science B.V., Amsterdam, 1995), Vol. 1A, p. 691.
- [28] K. Simons and E. Ikonen, Nature (London) **387**, 569 (1997).
- [29] K. Farsad and P. De Camilli, Current Opinion in Cell Biology **15**, 372 (2003).
- [30] D. R. Klopfenstein, M. Tomishige, N. Stuurman, and R. D. Vale, Cell **109**, 347 (2002).
- [31] B. J. Peter *et al.*, Science **303**, 495 (2004).